

# DiffusionXRay: A Diffusion and GAN-Based Approach for Enhancing Digitally Reconstructed Chest Radiographs

Aryan Goyal<sup>1†</sup>, Ashish Mittal<sup>2†</sup>, Pranav Rao<sup>2</sup>, Manoj Tadepalli<sup>2</sup>, and Preetham Putha<sup>2</sup>

<sup>1</sup> Indian Institute of Technology Bombay, India  
21d180006@iitb.ac.in

<sup>2</sup> Qure.ai, India

ashish.mittal@qure.ai, pranav.rao@qure.ai, manoj.tadepalli@qure.ai,  
preetham.putha@qure.ai

**Abstract.** Deep learning-based automated diagnosis of lung cancer has emerged as a crucial advancement that enables healthcare professionals to detect and initiate treatment earlier. However, these models require extensive training datasets with diverse case-specific properties. High-quality annotated data is particularly challenging to obtain, especially for cases with subtle pulmonary nodules that are difficult to detect even for experienced radiologists. This scarcity of well-labeled datasets can limit model performance and generalization across different patient populations. Digitally reconstructed radiographs (DRR) using CT-Scan to generate synthetic frontal chest X-rays with artificially inserted lung nodules offers one potential solution. However, this approach suffers from significant image quality degradation, particularly in the form of blurred anatomical features and loss of fine lung field structures. To overcome this, we introduce DiffusionXRay, a novel image restoration pipeline for Chest X-ray images that synergistically leverages denoising diffusion probabilistic models (DDPMs) and generative adversarial networks (GANs). DiffusionXRay incorporates a unique two-stage training process: First, we investigate two independent approaches, DDPM-LQ and GAN-based MUNIT-LQ, to generate low-quality CXRs, addressing the challenge of training data scarcity, posing this as a style transfer problem. Subsequently, we train a DDPM-based model on paired low-quality and high-quality images, enabling it to learn the nuances of X-ray image restoration. Our method demonstrates promising results in enhancing image clarity, contrast, and overall diagnostic value of chest X-rays while preserving subtle yet clinically significant artifacts, validated by both quantitative metrics and expert radiological assessment.

**Keywords:** Chest X-rays · Image Enhancement · Diffusion Models · Super-resolution · Medical Imaging.

---

\* † Equal contribution: Aryan Goyal and Ashish Mittal.

## 1 Introduction

Lung cancer, the fifth most common cancer worldwide [18], is often diagnosed late due to minimal early symptoms, impacting survival rates [5]. Although low-dose computed tomography (LDCT) is the preferred screening method for lung cancer [15], chest X-Rays are a widely used alternative due to lower radiation exposure and cost effectiveness. Despite their accessibility, chest X-rays pose challenges in early stage lung cancer detection due to subtle nodules and image variability. Automated nodule detection using deep learning has shown promise in supporting radiologists with early-stage identification in chest X-rays [3]. However, the scarcity of high-quality annotated chest X-ray data remains a major bottleneck in the development of reliable deep learning algorithms.

To mitigate data scarcity, digitally reconstructed radiographs (DRRs) from CT scans provide a scalable solution [14]. However, DRRs suffer from poor contrast, loss of fine structures, and reconstruction artifacts, limiting their diagnostic value. Enhancing DRRs while preserving subtle nodules and fine details is essential for improving lung cancer detection.

The lack of extensive datasets containing paired low-quality X-rays (DRRs)\* and high-quality X-ray images is a major limitation in training image enhancement models [11, 7]. A common approach to generating paired datasets is bicubic interpolation [17, 20], but it fails to replicate the complex degradations present in real low-quality X-rays, leading to poor generalization. Our experimental findings confirm this limitation, highlighting the need for more effective methods to create realistic paired data that accurately capture the unique degradations observed in real low-quality DRRs. To address this, several approaches have attempted to generate degraded images [16, 21, 23], with some treating the problem as an unsupervised domain adaptation task.

Single-image super-resolution (SISR) is a well-studied topic, with deep learning-based methods ranging from convolutional neural networks (CNNs) to Transformers [22, 2] and diffusion models [20, 9]. Recent diffusion models have outperformed GANs in image super-resolution, producing high-fidelity images with fine-grained details [12]. In the medical domain, however, applying these methods to MRI and X-ray data remains limited.

Our experience with existing models such as SwinIR [10] showed that while they produce sharp high resolution X-Rays, they often fail to preserve clinically significant details, such as subtle nodules or bone intersections. SwinFIR [22] improved global structure retention, but subtle nodules remained faded or distorted. Weber et al. [20] proposed a super-resolution DDPM trained on the MaChex dataset [20], but it focuses on super-resolution of low resolution X-Rays generated from another diffusion model which do not exhibit realistic degradation observed in DRRs.

---

\* Throughout this work, 'real low-quality X-rays' refers specifically to Digitally Reconstructed Radiographs (DRRs) obtained via CT projections, while 'generated low-quality X-rays' refer to images synthesized via MUNIT-LQ and DDPM-LQ, designed to mimic DRR degradations.

To address these challenges, We take a novel approach by reframing this problem as a style transfer task—preserving the overall structure while introducing degradations characteristic of low-quality CXRs. Unlike conventional image processing techniques, which struggle to replicate such degradations, our approach transfers them directly from LQ CXRs to HQ CXRs.

We introduce DiffusionXRay, which employs two independent methods to generate realistic paired data: (i) MUNIT-LQ, an adaptation of the MUNIT [6] framework, and (ii) DDPM-LQ, a diffusion-based model for learning complex degradations.

Our proposed method introduces the following novelties:

1. To address the lack of accurately paired high- and low-quality training data, we introduce a style transfer approach alongside unsupervised domain transfer. We evaluate two independent methods: (i) MUNIT-LQ (Multimodal Unsupervised Image-to-Image Translation) and (ii) DDPM-LQ, using a two-stage training process.
2. We train a DDPM on the paired dataset generated using MUNIT-LQ and DDPM-LQ, ensuring realistic degradations and subtle nodules. Both quantitative metrics and expert radiologist evaluations confirm that our model effectively preserves fine anatomical structures, including bronchial details and subtle pulmonary nodules.
3. We release a dataset of 12,580 low-quality chest X-rays generated from CT projections. Additionally, we provide two low-quality versions of the Chest X-ray [19] test split (25,596 images), generated using our proposed methods.

## 2 Methodology

### 2.1 Datasets

We introduce LQ-CXR12K (Low-Quality Chest X-ray dataset), comprising 12,580 low-quality chest X-rays generated via projection from low-dose CT scans sourced from our institutional dataset.

The MUNIT-LQ training used unpaired data comprising 15,000 high-quality chest X-ray images from our institutional dataset, SubtleNodules-CXR, specifically selected to contain solitary subtle nodules. For the unpaired LQ component, we employ LQ-CXR12K.

The baseline enhancement model was trained on paired datasets, where the low-quality counterpart was generated using bicubic downsampling on Machex Dataset [20]. While, the final enhancement model (DDPM-HQ) was trained on the in-house dataset of 300,000 images (HQ-CXR300K), where the degraded images were generated using MUNIT-LQ.

For evaluation, we utilize the ChestX-ray8 [19] test set containing 25,596 high-quality images. We generate low-quality counterparts using three distinct approaches: bicubic interpolation, MUNIT-LQ, and our DDPM-LQ as illustrated in Fig. 2. We release these generated low-quality sets along with their high-quality originals to facilitate future research and benchmarking.

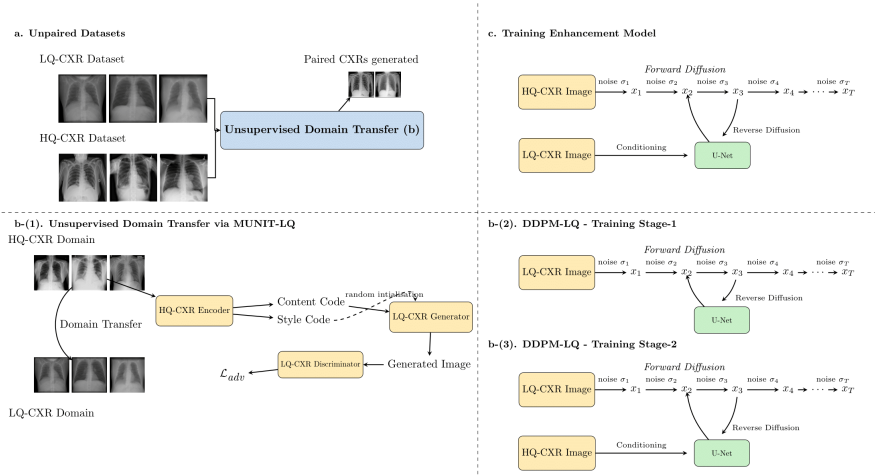


**Fig. 1.** Overview of our proposed DiffusionXRay framework. (a) Unpaired high and low-quality (CXRs) serve as training data for our unsupervised domain transfer models. (b) Implementation of domain transfer using: (b-1) MUNIT-LQ for style-guided translation or (b-2) DDPM-LQ for diffusion-based degradation modeling using 2 stage training. (c) The paired data generated from these models is subsequently used to train our final enhancement network which is DDPM-HQ.

## 2.2 Synthesizing Chest X-Ray via Projection from CT Scans

Synthetic frontal chest X-rays can be generated using ray tracing and Beer’s Law applied to CT scans with and without randomly inserted lung nodules, providing a diverse training dataset [13].

However, these digitally reconstructed radiographs (DRRs) suffer from blurred anatomical features and loss of fine lung structures. Degradations arise from noise artifacts (e.g., Gaussian noise, beam hardening, streak artifacts, motion distortions) in the CT volume and reconstruction artifacts introduced during the inverse Radon transformation, which converts sinogram data into volumetric images [1]. These distortions hinder the detection of subtle pulmonary abnormalities such as nodules and lesions, as they cannot be accurately simulated using simple degradations like bicubic interpolation or Gaussian filtering.

To address this, our pipeline employs MUNIT-LQ and DDPM-LQ to generate realistic low-quality counterparts, enabling the training of an enhancement model that refines DRRs into high-fidelity X-ray images suitable for deep learning applications.

## 2.3 MUNIT-LQ

The Multimodal Unsupervised Image-to-Image Translation (MUNIT)[6] framework implements image translation through disentangled representation via decomposing images into content and style codes. This enables example-guided

translation without requiring paired data—making it ideal for generating low-quality chest radiographs (CXRs) from high-quality inputs by leveraging our unpaired HQ-CXR and LQ CXR datasets for training. The translation process consists of two key steps. First, the content encoder extracts domain-invariant features from the HQ-CXR input images, generating a content code that preserves the essential structural information. Second, this content code is combined with a style code, which can either be randomly sampled from the target domain’s style space or derived from a user-provided example image.

MUNIT-LQ employs two generative adversarial networks:  $\text{GAN}_1 = \{D_1, G_1\}$  and  $\text{GAN}_2 = \{D_2, G_2\}$  each trained to reconstruct images within their respective domains i.e high quality CXRs for  $\text{GAN}_1$  and low quality CXRs for  $\text{GAN}_2$ .  $G_1$  is employed to generate low-quality CXRs from the translation stream  $\tilde{x}_2^{2 \rightarrow 1} = G_1(z_2 \sim q_2(z_2|x_2))$ . Adversarial training is performed on translated images  $\tilde{x}_2^{2 \rightarrow 1}$ .

*Loss Functions* The model optimizes a composite loss function comprising adversarial and reconstruction losses. The total loss is defined as:

$$\begin{aligned} \mathcal{L} = & \mathcal{L}_{x1_{GAN}} + \mathcal{L}_{x2_{GAN}} + \lambda_x(\mathcal{L}_{x1_{recon}} + \mathcal{L}_{x2_{recon}}) \\ & + \lambda_c(\mathcal{L}_{c1_{recon}} + \mathcal{L}_{c2_{recon}}) + \lambda_s(\mathcal{L}_{s1_{recon}} + \mathcal{L}_{s2_{recon}}) \end{aligned} \quad (1)$$

where the image reconstruction loss is computed as:

$$\mathcal{L}_{x1_{recon}} = \mathbb{E}_{x1 \sim p(x1)} [\|G_1(E_1^c(x1), E_1^s(x1)) - x1\|_1] \quad (2)$$

The content and style reconstruction losses are given by:

$$\mathcal{L}_{c1_{recon}} = \mathbb{E}_{c1 \sim p(c1), s2 \sim q(s2)} [\|E_2^c(G_2(c1, s2)) - c1\|_1] \quad (3)$$

$$\mathcal{L}_{s2_{recon}} = \mathbb{E}_{c1 \sim p(c1), s2 \sim q(s2)} [\|E_2^s(G_2(c1, s2)) - s2\|_1] \quad (4)$$

The adversarial loss ensures the translated images match the target domain distribution:

$$\mathcal{L}_{x2_{GAN}} = \mathbb{E}_{c1 \sim p(c1), s2 \sim q(s2)} [\log(1 - D_2(G_2(c1, s2)))] + \mathbb{E}_{x2 \sim p(x2)} [\log D_2(x2)] \quad (5)$$

where  $\lambda_x$ ,  $\lambda_c$ , and  $\lambda_s$  are weighting parameters that balance the contribution of each reconstruction term.

In addition to MUNIT’s standard loss functions, we use a domain-invariant perceptual loss via a pre-trained VGG network[8] and a cyclic consistency loss[24].

## 2.4 DDPM

Diffusion Probabilistic Models (DDPMs) outperform GANs in preserving fine anatomical details due to their iterative denoising process and flexible conditioning mechanisms. These properties provide precise control over both the generation process and output characteristics, making DDPMs well-suited for both image enhancement and degradation modelling. Our image enhancement model

and DDPM-LQ are based on the conditional DDPM framework [4]. DDPMs approximate data distributions  $p(x_0)$  through a forward process that progressively adds Gaussian noise according to a variance schedule  $\beta_t$ , transforming a data point  $x_0$  into a sequence of increasingly noisy latents  $x_1, \dots, x_T$ :

$$q(x_t|x_{t-1}) = \mathcal{N}(x_t; \sqrt{1 - \beta_t}x_{t-1}, \beta_t\mathbf{I}) \quad (6)$$

The reverse process learns to remove noise step-by-step, approximating the true data distribution via a probabilistic model:

$$p_\theta(x_{t-1}|x_t) = \mathcal{N}(x_{t-1}; \mu_\theta(x_t, t), \Sigma_\theta(x_t, t))$$

where the mean  $\mu_\theta$  and variance  $\Sigma_\theta$  are parameterized by a neural network, typically a U-Net, which predicts the noise component  $\epsilon_\theta(x_t, t)$ . The reverse process gradually reconstructs the original data by iteratively denoising the latents.

For generating low-quality counterparts from high-quality CXRs, DDPM-LQ generates samples from its learned distribution. We initialize our approach using the pre-trained checkpoint from Weber et al. [20], which also serves as our baseline. We employ a two-stage training procedure:

1. **Unconditional DDPM Training** – In the first stage, we train DDPM-LQ on 160k real low-quality images -LQ-CXR160K, derived from CT scan projections to learn low-quality characteristics.
2. **Conditional Fine-Tuning** – The second stage involves fine-tuning on 300k paired HQ-LQ images, where HQ-CXRs are used as conditioning inputs concatenated with the noise latent during training. The LQ CXR component of the paired dataset was generated using MUNIT-LQ and bicubic downsampling applied on the HQ-CXR300K dataset

This two-stage approach ensures the model learns both general low-quality characteristics and the ability to generate corresponding low-quality images conditioned on high-quality inputs. Finally, our enhancement model is trained on a dataset of 300k paired CXRs, incorporating synthetic low-quality images from DDPM-LQ and MUNIT-LQ.

## 3 Experiments

### 3.1 Setup

The DiffusionXRay training pipeline is essentially a 2-step procedure, the first step being the generation of LQ counterpart given a HQ CXR input, using DDPM-LQ or MUNIT-LQ trained on unpaired datasets: LQ-CXR and HQ-CXR datasets. In the second step we leverage this generated paired dataset to train enhancement models, we employ to train DDPM-based enhancement models. The final enhancement model is then evaluated on the ChestX-ray8[19] dataset with the low quality X-rays generated using MUNIT-LQ and DDPM-LQ using PSNR and SSIM scores and qualitative evaluation by expert radiologists against the baseline enhancement model.

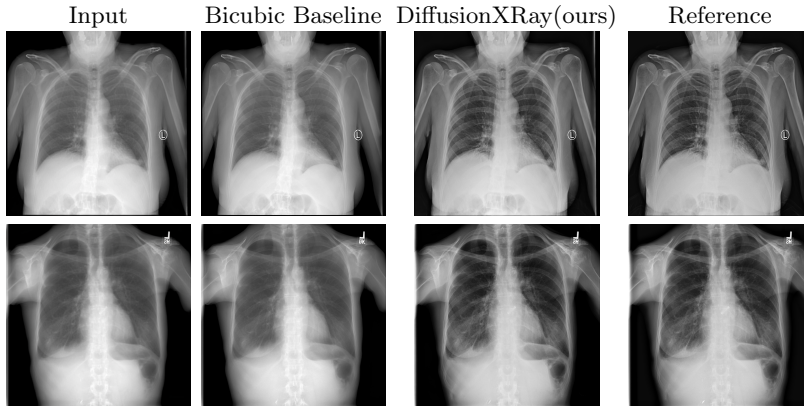


**Fig. 2.** Qualitative comparison of image enhancement and super-resolution results ( $512 \times 512 \rightarrow 1024 \times 1024$ ) on synthetically degraded chest X-ray (CXR) images. Each input image was a high-quality (HQ) CXR artificially degraded using the MUNIT-LQ framework. The bicubic baseline refers to a DDPM model trained on paired data generated with bicubic downsampling. The reference shown is the original HQ-CXR.

### 3.2 Results

**Automated metrics** Quantitatively as shown in Table 1, DiffusionXRay outperforms the bicubic interpolation low-quality data baseline on PSNR and SSIM. As illustrated in Fig.2, DiffusionXRay produces superior contrast and clarity, whereas the bicubic interpolation baseline DDPM still retains blur and haze artifacts.

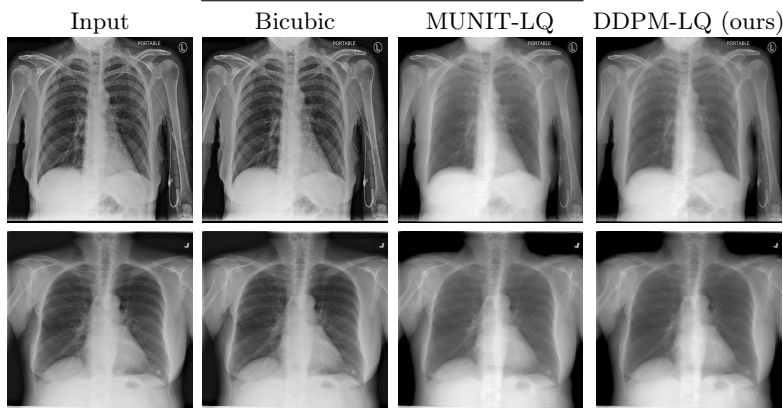
**Table 1.** Quantitative comparison on  $512 \times 512 \rightarrow 1024 \times 1024$  super-resolution and enhancement with low-quality data generated via MUNIT-LQ and DDPM-LQ on ChestX-ray8[19] dataset.

Results with MUNIT-LQ generated data		
Metric	Bicubic-DDPM Model	Diffusion-Xray (Ours)
PSNR $\uparrow$	20.08	<b>27.50</b>
SSIM $\uparrow$	0.83	<b>0.92</b>
Results with DDPM-LQ generated data		
PSNR $\uparrow$	19.85	<b>22.21</b>
SSIM $\uparrow$	0.78	0.78

**Human Evaluation** Quantitative metrics indicate improvement but fail to adequately capture nodule preservation and clinically significant features. Therefore, we employed radiologist-based mean opinion scores (MOS) to assess nodule visibility and overall image quality, with emphasis on lung field clarity.

**Table 2.** Qualitative comparison for nodule reservation and overall quality assessment by expert radiologists for CXR enhancement

<b>Task 1</b>	<b>Q1 ↑</b>	<b>Q2 ↓</b>
DiffusionXRay (ours)	<b>100%</b>	<b>0%</b>
Bicubic-DDPM	6.6%	30%
<b>Task 2</b>	<b>Q1 ↑</b>	<b>Q2 ↓</b>
DiffusionXRay (ours)	<b>100%</b>	<b>72.9%</b>
Bicubic-DDPM	66.7%	<b>25%</b>

**Fig. 3.** Qualitative comparison of low-quality CXR synthesis from high-quality CXRs using bicubic interpolation, MUNIT-LQ, and DDPM-LQ.

In Task 1 (nodule preservation), radiologists reviewed a low-quality input alongside two enhanced outputs—one from bicubic interpolation and one from our model—with nodules highlighted by bounding boxes. They answered:

1. Q1 - "Is the nodule easily visible in the post-processed image?"
2. Q2 - "Could the nodule in the post-processed image be confused with other structures (e.g., bones, artifacts, leads, or buttons)?"

For Task 2 (quality assessment), radiologists evaluated:

1. Q1 - "Has the clarity of the lung fields improved compared to the original projected image?"
2. Q2 - "Is there a significant increase in noise in the lung fields?"

Each evaluation used triplets of images, comprising an original CT-projected image and two blinded post-processed versions. As Table 2 demonstrates, our model significantly outperforms the baseline in both tasks, despite introducing some noise patterns, as indicated in Task 2 responses.

## 4 Conclusion

We introduce DiffusionXRay, an image enhancement pipeline for digitally reconstructed radiographs (DRRs) from CT scans, addressing the challenge of subtle

feature distortion and contrast loss. By constructing realistic training pairs using MUNIT-LQ and DDPM-LQ, we overcome a key bottleneck in enhancement model training.

Qualitative and quantitative evaluations confirm significant improvements, validating DiffusionXRay as a viable data augmentation tool. However, its high computational cost remains a limitation, which future work could mitigate by improving efficiency and exploring adaptive conditioning for selective feature preservation. Beyond DRRs, DiffusionXRay can be adapted to other tasks such as portable X-rays enhancement. Future research could refine the approach to enhance X-rays across varying acquisition conditions while maintaining diagnostic integrity.

**Disclosure of Interests:** The authors have no competing interests to declare that are relevant to the content of this paper.

## References

1. Benning, M., Burger, M.: Modern regularization methods for inverse problems. *Acta Numerica* **27**, 1–111 (2018). <https://doi.org/10.1017/S0962492918000016>
2. Chen, X., Wang, X., Zhou, J., Qiao, Y., Dong, C.: Activating more pixels in Image Super-Resolution Transformer (5 2022), <https://arxiv.org/abs/2205.04437>
3. Hendrix, W., Hendrix, N., Scholten, E.T., Mourits, M., Jong, J.T.D., Schalekamp, S., Korst, M., Van Leuken, M., Van Ginneken, B., Prokop, M., Rutten, M., Jacobs, C.: Deep learning for the detection of benign and malignant pulmonary nodules in non-screening chest CT scans. *Communications Medicine* **3**(1) (10 2023). <https://doi.org/10.1038/s43856-023-00388-5>, <https://doi.org/10.1038/s43856-023-00388-5>
4. Ho, J., Jain, A., Abbeel, P.: Denoising diffusion probabilistic models (2020), <https://arxiv.org/abs/2006.11239>
5. Howlader, N., Noone, A.M., Krapcho, M., Miller, D., Bishop, K., Kosary, C.L., Yu, M., Ruhl, J., Tatalovich, Z., Mariotto, A., Lewis, D.R., Chen, H.S., Feuer, E.J., Cronin, K.A.: Seer cancer statistics review, 1975-2014 (2017), [https://seer.cancer.gov/csr/1975\\_2014/](https://seer.cancer.gov/csr/1975_2014/), based on November 2016 SEER data submission, posted to the SEER web site, April 2017
6. Huang, X., Liu, M.Y., Belongie, S., Kautz, J.: Multimodal unsupervised image-to-image translation (2018), <https://arxiv.org/abs/1804.04732>
7. Ji, X., Cao, Y., Tai, Y., Wang, C., Li, J., Huang, F.: Real-world super-resolution via kernel estimation and noise injection. In: *The IEEE/CVF Conference on Computer Vision and Pattern Recognition (CVPR) Workshops* (June 2020)
8. Johnson, J., Alahi, A., Fei-Fei, L.: Perceptual losses for real-time style transfer and super-resolution (2016), <https://arxiv.org/abs/1603.08155>
9. Li, H., Yang, Y., Chang, M., Feng, H., Xu, Z., Li, Q., Chen, Y.: SRDiff: Single Image Super-Resolution with Diffusion Probabilistic Models (4 2021), <https://arxiv.org/abs/2104.14951>
10. Liang, J., Cao, J., Sun, G., Zhang, K., Luc, V.G., Timofte, R.: SWiNIR: Image restoration using SWIN Transformer (8 2021), <https://arxiv.org/abs/2108.10257>
11. Lugmayr, A., Danelljan, M., Timofte, R.: Unsupervised learning for real-world super-resolution (2019), <https://arxiv.org/abs/1909.09629>

12. Moser, B.B., Shanbhag, A.S., Raue, F., Frolov, S., Palacio, S., Dengel, A.: Diffusion models, image super-resolution and everything: A survey (2024), <https://arxiv.org/abs/2401.00736>
13. Moturu, A., Chang, A.: Creation of synthetic x-rays to train a neural network to detect lung cancer (2018), <https://api.semanticscholar.org/CorpusID:52972967>
14. Moturu, A., Chang, A., Department of Computer Science, U.o.T.: Creation of synthetic X-Rays to train a neural network to detect lung cancer. Tech. rep., University of Toronto (8 2018), [https://www.cs.toronto.edu/pub/reports/na/Project\\_Report\\_Moturu\\_Chang\\_1.pdf](https://www.cs.toronto.edu/pub/reports/na/Project_Report_Moturu_Chang_1.pdf)
15. null null: Reduced lung-cancer mortality with low-dose computed tomographic screening (2011). <https://doi.org/10.1056/NEJMoa1102873>, <https://www.nejm.org/doi/full/10.1056/NEJMoa1102873>
16. Peng, L., Li, W., Pei, R., Ren, J., Fu, X., Wang, Y., Cao, Y., Zha, Z.J.: Towards realistic data generation for real-world super-resolution (2024), <https://arxiv.org/abs/2406.07255>
17. Saharia, C., Ho, J., Chan, W., Salimans, T., Fleet, D.J., Norouzi, M.: Image super-resolution via iterative refinement (2021), <https://arxiv.org/abs/2104.07636>
18. Sung, H., Ferlay, J., Siegel, R.L., Laversanne, M., Soerjomataram, I., Jemal, A., Bray, F.: Global Cancer Statistics 2020: GLOBOCAN estimates of incidence and mortality worldwide for 36 cancers in 185 countries. *CA A Cancer Journal for Clinicians* **71**(3), 209–249 (2 2021). <https://doi.org/10.3322/caac.21660>, <https://pubmed.ncbi.nlm.nih.gov/33538338/>
19. Wang, X., Peng, Y., Lu, L., Lu, Z., Bagheri, M., Summers, R.: Chestx-ray8: Hospital-scale chest x-ray database and benchmarks on weakly-supervised classification and localization of common thorax diseases. In: 2017 IEEE Conference on Computer Vision and Pattern Recognition (CVPR). pp. 3462–3471 (2017)
20. Weber, T., Ingrisch, M., Bischl, B., Rügamer, D.: Cascaded Latent Diffusion Models for High-Resolution Chest X-ray Synthesis (3 2023), <https://arxiv.org/abs/2303.11224>
21. Yang, T., Ren, P., Xie, X., Zhang, L.: Synthesizing Realistic Image Restoration Training pairs: a diffusion approach (3 2023), <https://arxiv.org/abs/2303.06994>
22. Zhang, D., Huang, F., Liu, S., Wang, X., Jin, Z.: SwinFIR: Revisiting the SwinIR with Fast Fourier Convolution and Improved Training for Image Super-Resolution (8 2022), <https://arxiv.org/abs/2208.11247>
23. Zhang, K., Liang, J., Gool, L.V., Timofte, R.: Designing a practical degradation model for deep blind image super-resolution (2021), <https://arxiv.org/abs/2103.14006>
24. Zhu, J.Y., Park, T., Isola, P., Efros, A.A.: Unpaired image-to-image translation using cycle-consistent adversarial networks (2020), <https://arxiv.org/abs/1703.10593>